nature geoscience

LETTERS

PUBLISHED ONLINE: 31 AUGUST 2015 | DOI: 10.1038/NGEO2517

Two distinct influences of Arctic warming on cold winters over North America and East Asia

Jong-Seong Kug[1], Jee-Hoon Jeong[2*], Yeon-Soo Jang[1], Baek-Min Kim[3], Chris K. Folland[4,5], Seung-Ki Min[1] and Seok-Woo Son[6]

Arctic warming has sparked a growing interest because of its possible impacts on mid-latitude climate[1–5]. A number of unusually harsh cold winters have occurred in many parts of East Asia and North America in the past few years[2,6,7], and observational and modelling studies have suggested that atmospheric variability linked to Arctic warming might have played a central role[1,3,4,8–11]. Here we identify two distinct influences of Arctic warming which may lead to cold winters over East Asia or North America, based on observational analyses and extensive climate model results. We find that severe winters across East Asia are associated with anomalous warmth in the Barents–Kara Sea region, whereas severe winters over North America are related to anomalous warmth in the East Siberian–Chukchi Sea region. Each regional warming over the Arctic Ocean is accompanied by the local development of an anomalous anticyclone and the downstream development of a mid-latitude trough. The resulting northerly flow of cold air provides favourable conditions for severe winters in East Asia or North America. These links between Arctic and mid-latitude weather are also robustly found in idealized climate model experiments and CMIP5 multi-model simulations. We suggest that our results may help improve seasonal prediction of winter weather and extreme events in these regions.

One of the clearest manifestations of recent climate change is Arctic amplification—that is, surface warming over the Arctic being faster than that at other latitudes under greenhouse warming[12]. Such amplification has accelerated in recent decades and the Arctic has warmed approximately twice as rapidly as the Northern Hemisphere (NH) as a whole[5]. This clearly indicates that the Arctic is very susceptible to climate change, a phenomenon evident in both observations and climate projections[12,13].

Although greenhouse gas concentrations have increased continuously over the past half-century, extratropical NH winter temperature trends have exhibited considerable interdecadal variation (Fig. 1), partly because of natural climate variability. For example, between 1979 and 1997, when global-mean surface air temperature (SAT) increase was fastest, the winter warming trend was clear over Europe, East Asia and the USA (Fig. 1a), whereas the Arctic exhibited little trend or even slight cooling in places. However, between 1998 and 2013, the pattern of winter SAT trends in these regions became conspicuously different from that in 1979–1997. First, Arctic surface warming has progressed rapidly since 1998 (Fig. 1b), with stronger warming trends over the Barents–Kara and East Siberian–Chukchi sea regions where marked reductions in sea-ice concentration have occurred[12]. By contrast, strong cooling trends are evident over parts of the extratropical northern continents[3,14]. In addition to these cooling trends, many parts of the northern continents have experienced frequent cold extremes, especially in recent years[2,6,7].

A key feature of Fig. 1 is the generally opposite sign of SAT trends between the Arctic and extratropics in the two epochs; in the earlier epoch the Arctic was actually cooling slightly whereas in the later epoch it was warming rapidly. Many recent studies have suggested that recent cold winters in northern continents are related to Arctic warming[5,8–11,15–18]. However, it remains debatable whether the trend to colder winters is due to Arctic amplification or internal variability[2,5,19–21] because the underlying dynamical mechanisms are not fully understood. Several studies have argued that sea-ice loss over the Barents–Kara Sea region in autumn plays a critical role in influencing atmospheric circulation in the following

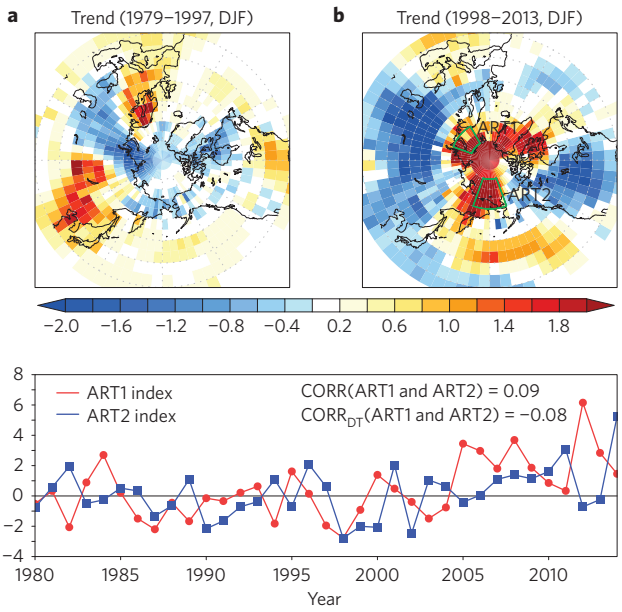

Figure 1 | SAT trends and Arctic temperature (ART) indices. a,**b**, The linear trend in surface air temperature during December–February for the periods 1979/1980–1997/1998 (**a**) and 1997/1998–2013/2014 (**b**) from the observed data[32]. Green boxes denote the region for ART indices in **b**. **c**, Time series of seasonal-mean ART1 and ART2 during December–February for the period 1979/1980–2013/2014. DT denotes the de-trended state.

[1]School of Environmental Science and Engineering, Pohang University of Science and Technology (POSTECH), 37673 Pohang, Korea. [2]Department of Oceanography, Chonnam National University, 61186 Gwangju, Korea. [3]Korea Polar Research Institute, 21990 Incheon, Korea. [4]Met Office Hadley Centre, Exeter EX1 3PB, UK. [5]Department of Earth Sciences, University of Gothenburg, 405 30 Gothenburg, Sweden. [6]School of Earth and Environmental Sciences, Seoul National University, 00826 Seoul, Korea. *e-mail: jjeehoon@jnu.ac.kr

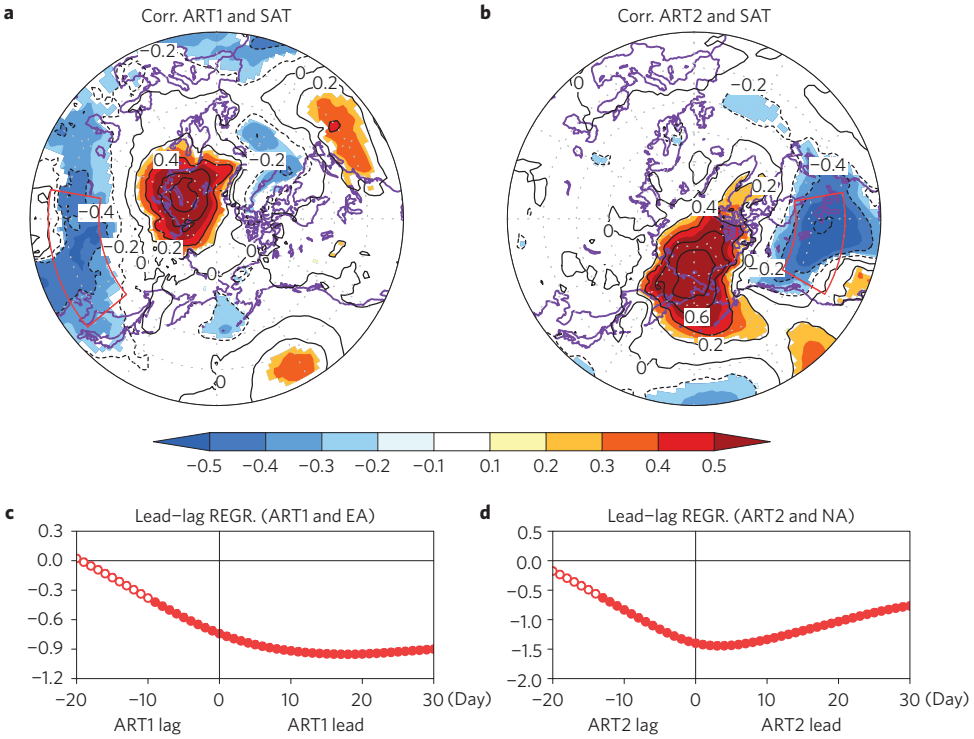

Figure 2 | Relationships between Arctic temperature and SAT over the NH extratropics. a,**b**, Correlation coefficients of SAT anomalies with respect to de-trended monthly ART1 (**a**) and ART2 indices (**b**) during December–February for the period 1979/1980–2013/2014 from the reanalysis data. Shading denotes significant values at the 95% confidence level based on a Student's *t*-test. **c**,**d**, Lead–lag regression coefficients of a moving 31-day-mean SAT over East Asia (80°–130° E, 35°–50° N) with respect to the normalized ART1 index (**c**), and over North America (80°–120° W, 40°–55° N) with respect to the normalized ART2 index (**d**). Correlation coefficients that are statistically significant at the 95% confidence level are indicated with filled circles.

winter[11,17,18,22–24]. A reduction of autumn sea ice is generally followed by warm Arctic SAT in winter (Supplementary Figs 3 and 4). This often leads to the so-called 'warm Arctic–cold continent' pattern[23] forced via stationary Rossby waves[11]. It is further suggested that more frequent and persistent episodes of atmospheric blocking occur[10,15,17], with downstream responses of enhanced cyclonic activity[9,18] and possibly weakening of the polar vortex due to an enhanced upward propagation of planetary waves[8]. Accordingly, Arctic sea-ice information may be useful for improving climate prediction in NH extratropical regions[25]. However, atmospheric responses to Arctic sea-ice variations are complex, depending on background atmospheric states and seasons[9,22], which may weaken statistical relationships with extratropical climate variations. Furthermore, it has recently been recognized that extratropical impacts depend highly on the regional structure of the anomalous Arctic climate state[16,26].

In high latitudes, surface heat flux forcing and low-level baroclinicity associated with sea-ice loss and other anomalous Arctic climate states are important for modulating the slow-varying atmospheric circulation[8,18,22]. Modelling studies showed that these sea-ice variations are related to regional SAT patterns[17,21,22] that are easy to observe and have relatively high predictability. To investigate the observed connections between Arctic warming and regional extratropical cold winters, we define two Arctic temperature (ART) indices: ART1, which averages SAT over the Barents–Kara Sea region (30°–70° E, 70°–80° N), and ART2, which averages SAT over the East Siberian–Chukchi Sea region (160° E–160° W, 65°–80° N). These two regions exhibit the strongest warming trends since 1998 (Fig. 1b), but de-trended correlations between the two indices are almost zero (Fig. 1c).

Figure 2 shows correlations between the de-trended monthly ART indices and SAT from 1979 to 2014. Both indices exhibit strong positive correlations over their own regions, but show different correlation patterns in much of the NH extratropics. For ART1, negative correlations prevail over most of Eurasia (Fig. 2a), and are particularly strong over East Asia. This indicates that when the Arctic SAT gets warmer over the Barents–Kara Sea region, East Asia experiences cold winters, consistent with previous studies[9,11,18].

On the other hand, the ART2 index is negatively correlated with SAT anomalies over North America (Fig. 2b). The negative correlation is strongest over most of Canada and the central and eastern parts of the United States. The correlation coefficient between monthly ART2 and North American SAT in the region shown in Fig. 2b is close to −0.65, suggesting that North American winter SAT anomalies are strongly negatively correlated with SAT anomalies in the East Siberian–Chukchi Sea region. These relationships are fairly robust even for long-term historical data (Supplementary Fig. 2).

Figure 2c,d shows lead–lag relationships between the ART indices and East Asian and North American SAT calculated from a moving 31-day-mean ERA-Interim data set[27]. As shown in Fig. 2c,d, ART1 tends to precede the maximum East Asian SAT response by about 15 days, and ART2 shows the strongest relationship with North America SAT, about 5 days ahead. These results imply that the atmospheric circulation anomalies associated with the continental cooling over both regions are related to the regional Arctic warming in the upstream regions, suggesting that regional patterns of Arctic warming/cooling may be crucial for understanding extratropical NH winter climate variability.

Figure 3 shows the atmospheric circulation anomalies associated with regional Arctic warming. Warm conditions over the Barents–Kara Sea region (ART1) are associated with negative sea-level pressure (SLP) anomalies over the central Arctic and strong positive anomalies over western Russia (Fig. 3a). The positive SLP anomalies over western Russia develop from the coastal regions of the Barents–Kara Sea, slightly southward of the ART1 centre, to the central Eurasian continent. Once the anomalous anticyclonic

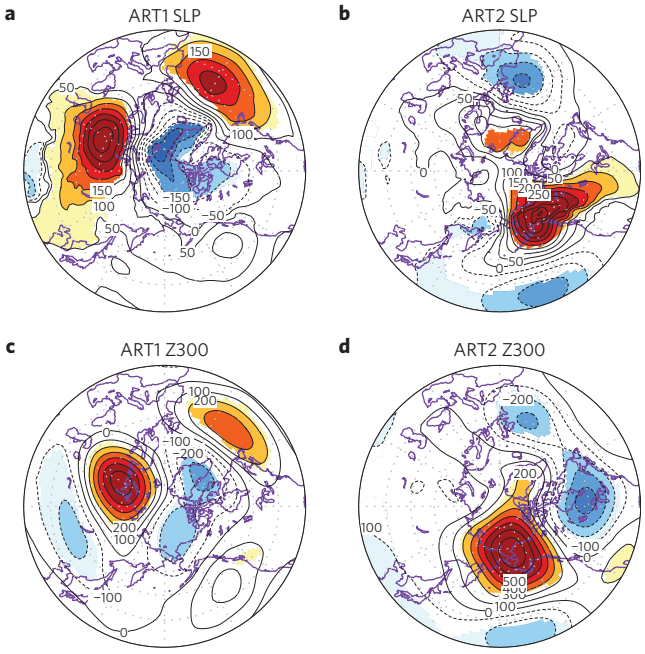

Figure 3 | Atmospheric circulation anomalies linked to Arctic temperature. Linear regression of sea-level pressure (Pa) (**a**,**b**) and 300 hPa geopotential height (m) (**c**,**d**) with respect to de-trended monthly ART1 (**a**,**c**) and ART2 indices (**b**,**d**) during December–February for the period of 1979/1980–2013/2014. Shading denotes significant values at 95% confidence level based on a Student's *t*-test.

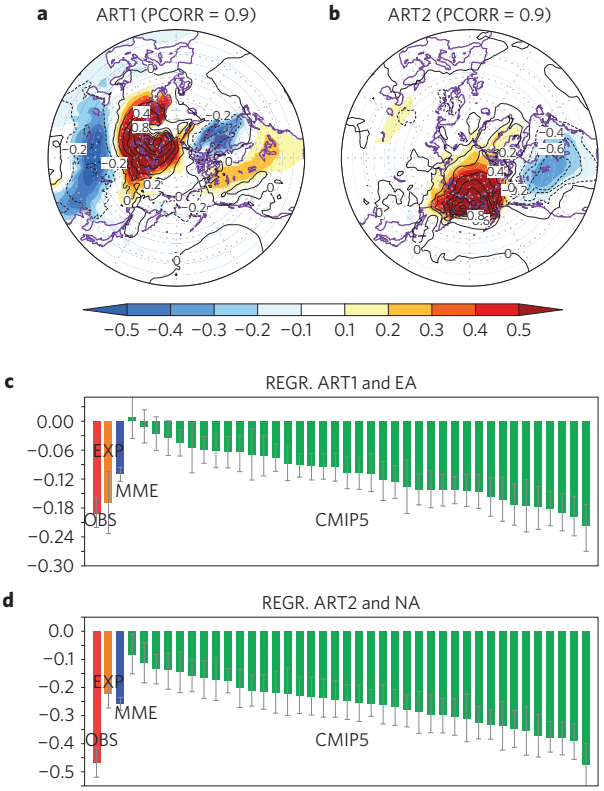

Figure 4 | Modelling support on the relationships between Arctic temperature and SAT over the NH extratropics. a,**b**, SAT anomalies regressed on de-trended monthly ART1 (**a**) and ART2 indices (**b**) during December–February for the period 1979/1980–2012/13 from observation (contour) and CM2.1 model experiments (shaded). The pattern correlation coefficients between the observation and the model experiments over 30°–90° N are denoted in the upper right side of the figure. **c**,**d**, Regression coefficients of SAT over the East Asia region on the ART1 index (**c**) and SAT over the North America region on the ART2 index (**d**) during December–February in the 39 CMIP5 simulations. Red and orange bars show the coefficients from the observation and the CM2.1 model experiments, respectively. Green bars show the coefficients from the CMIP5 models, and blue bars denote the multi-model ensemble mean. The scale bars represent a range of 95% confidence levels from internal variability using a Monte Carlo approach.

flow is established, it develops further and expands to the east owing to anomalous cold advection at the climatologically cold surface[28]. The eastward expansion of the anomalous west-Russian anticyclone is linked to an intensified Siberian High, leading to cold advection and frequent occurrence of cold events over East Asia[28,29]. It is noteworthy from Fig. 3a,c that significant positive anomalies appear over the North Atlantic, centred near 40° N, upstream of the ART1 region. Likewise, significant negative anomalies are evident over the subtropical North Pacific, upstream of the ART2 region. These statistical results suggest that regional Arctic warming and their downstream teleconnection patterns could be influenced by such upstream disturbances[30]. The role of the upstream disturbances in the Arctic-to-extratropical connections needs further study (for example, Supplementary Fig. 5).

The upper-level circulation shows that the anomalous west-Russian anticyclone is quasi-equivalent barotropic, and accompanies anomalous cyclonic flow in the downstream region of far eastern Siberia (Fig. 3c). This cyclonic anomaly can be explained by Rossby wave propagation from the upstream anticyclonic anomaly. Such an upper cyclonic anomaly implies an intensified and westward-shifted Asian trough, closely related to a stronger East Asian winter monsoon with more frequent cold extreme events[29].

Circulation patterns associated with ART2 are seemingly different from those with ART1. For example, the SLP responses over the Arctic are opposite. However, there is great dynamical similarity, particularly in the downstream regions. There is an anomalous equivalent barotropic anticyclone near the Arctic warming area and anomalous cyclonic flow in the downstream regions (Fig. 3b,d). The anomalous anticyclone implies a weakened Aleutian Low and more frequent North Pacific blocking events[31]. Associated northerly winds bring cold Arctic air into northern North America.

The above results clearly indicate that regional warming over the Arctic Ocean can affect extratropical climate in the downstream region by inducing a downstream teleconnection pattern. To substantiate the Arctic-to-extratropical connections in the observations, idealized model experiments were carried out using a coupled global climate model (GCM). In the six model experiments, sea surface temperature (SST) in the Arctic region was restored to the historical SST but the model was fully coupled with the oceans in other regions (see Methods). The sea-ice concentration simulated in the model mostly follows the observational evolution, indicating that sea ice quickly adjusts to the SST evolution.

For these model simulations, a similar correlation analysis of de-trended ART1 and ART2 with SAT is performed (Fig. 4a,b). Figure 4a shows that, for ART1, the model gives a similar pattern of negative correlation of SAT over the Eurasian continent, the negative correlation being again strong over East Asia. The pattern correlation between the observations and the model simulation is 0.90, indicating high similarity between model responses and the observations. More importantly, the model quantitatively reproduces the regression coefficient of the observations (compare red and orange bars in Fig. 4c). For ART2, the model simulation also captures the overall negative SAT correlation over northern North America well. The pattern correlation between the observation and model simulation is very high at 0.90, although regression coefficient is underestimated (Fig. 4d). In addition to the SAT pattern,

the model also simulates the observed downstream atmospheric teleconnection patterns reasonably well (Supplementary Fig. 6). Because only the high-latitude SST is restored to the observed SST in the model experiments, these results strongly support two separate Arctic influences on NH extratropical winter climate.

These results are further supported by an extensive multi-model analysis. Simulations from 39 CMIP5 (Coupled Model Intercomparison Project phase 5) models are analysed to examine the relationships between their own de-trended monthly ART indices and East Asian and North American SAT (Fig. 4c,d and also see Supplementary Figs 7 and 8). In general, the CMIP5 models reproduce the observed circulation anomalies associated with ART indices reasonably well (Supplementary Fig. 9). It is found that 36 out of 39 models show statistically significant negative regressions between the ART1 index and East Asian SAT, supporting the idea that warming over the Barents–Kara Sea region is connected to cooling over East Asia. However, most CMIP5 models underestimate the observed regression coefficients. For ART2, all CMIP5 models show statistically significant negative regressions, although most models again show smaller regression coefficients than observations (Fig. 4d). Although the most models consistently simulate the negative regression coefficients of SAT, there is a large inter-model diversity in their magnitude.

This study shows that there are two key Arctic regions where regional warming can induce distinguishable cold winters over northern continents. Warming over the Barents–Kara Sea region is likely to lead to East Asian cooling, whereas northern North America cooling is closely related to warming over the East Siberian–Chukchi Sea region. These results suggest that the regional distribution of Arctic warming may provide additional predictability for intra-seasonal to seasonal forecasts in the NH extratropics. These results may also provide guidance for assessing the potential risk of extreme events over regions where current seasonal prediction skill is often poor. In particular, this study suggests that the recent increased frequency of severe winters over East Asia and North America may be partly caused by recent rapid Arctic warming.

Methods

Methods and any associated references are available in the online version of the paper.

Received 16 February 2015; accepted 23 July 2015; published online 31 August 2015

References

1. Francis, J. A. & Vavrus, S. J. Evidence for a wavier jet stream in response to rapid Arctic warming. *Environ. Res. Lett.* **10,** 014005 (2015).
2. Wallace, J. M., Held, I. M., Thompson, D. W., Trenberth, K. E. & Walsh, J. E. Global warming and winter weather. *Science* **343,** 729–730 (2014).
3. Outten, S. D. & Esau, I. A link between Arctic sea ice and recent cooling trends over Eurasia. *Climatic Change* **110,** 1069–1075 (2012).
4. Screen, J. A. & Simmonds, I. Amplified mid-latitude planetary waves favour particular regional weather extremes. *Nature Clim. Change* **4,** 704–709 (2014).
5. Cohen, J. *et al.* Recent Arctic amplification and extreme mid-latitude weather. *Nature Geosci.* **7,** 627–637 (2014).
6. Van Oldenborgh, G. J., Haarsma, R., De Vries, H. & Allen, M. R. Cold extremes in North America vs. mild weather in Europe: The winter of 2013–14 in the context of a warming world. *Bull. Am. Meteorol. Soc.* **96,** 707–714 (2015).
7. Wang, L. & Chen, W. The East Asian winter monsoon: Re-amplification in the mid-2000s. *Chin. Sci. Bull.* **59,** 430–436 (2014).
8. Kim, B. M. *et al.* Weakening of the stratospheric polar vortex by Arctic sea-ice loss. *Nature Commun.* **5,** 4646 (2014).
9. Tang, Q. H., Zhang, X. J., Yang, X. H. & Francis, J. A. Cold winter extremes in northern continents linked to Arctic sea ice loss. *Environ. Res. Lett.* **8,** 014036 (2013).
10. Screen, J. A. & Simmonds, I. Exploring links between Arctic amplification and mid-latitude weather. *Geophys. Res. Lett.* **40,** 959–964 (2013).
11. Honda, M., Inoue, J. & Yamane, S. Influence of low Arctic sea-ice minima on anomalously cold Eurasian winters. *Geophys. Res. Lett.* **36,** L08707 (2009).
12. Hartmann, D. L. *et al.* in *Climate Change 2013: The Physical Science Basis* (eds Stocker, T. F. *et al.*) 159–254 (IPCC, Cambridge Univ. Press, 2013).
13. Simmonds, I. Comparing and contrasting the behaviour of Arctic and Antarctic sea ice over the 35-year period 1979–2013. *Ann. Glaciol.* **56,** 18–28 (2015).
14. Cohen, J. L., Furtado, J. C., Barlow, M., Alexeev, V. A. & Cherry, J. E. Asymmetric seasonal temperature trends. *Geophys. Res. Lett.* **39,** L04705 (2012).
15. Francis, J. A. & Vavrus, S. J. Evidence linking Arctic amplification to extreme weather in mid-latitudes. *Geophys. Res. Lett.* **39,** L06801 (2012).
16. Petoukhov, V. & Semenov, V. A. A link between reduced Barents–Kara sea ice and cold winter extremes over northern continents. *J. Geophys. Res.* **115,** D21111 (2010).
17. Liu, J., Curry, J. A., Wang, H., Song, M. & Horton, R. M. Impact of declining Arctic sea ice on winter snowfall. *Proc. Natl Acad. Sci. USA* **109,** 4074–4079 (2012).
18. Inoue, J., Hori, M. E. & Takaya, K. The Role of Barents Sea ice in the wintertime cyclone track and emergence of a warm-Arctic cold-Siberian anomaly. *J. Clim.* **25,** 2561–2568 (2012).
19. Screen, J. A., Deser, C., Simmonds, I. & Tomas, R. Atmospheric impacts of Arctic sea-ice loss, 1979–2009: Separating forced change from atmospheric internal variability. *Clim. Dynam.* **43,** 333–344 (2013).
20. Fischer, E. M. & Knutti, R. Heated debate on cold weather. *Nature Clim. Change* **4,** 537–538 (2014).
21. Mori, M., Watanabe, M., Shiogama, H., Inoue, J. & Kimoto, M. Robust Arctic sea-ice influence on the frequent Eurasian cold winters in past decades. *Nature Geosci.* **7,** 869–873 (2014).
22. Deser, C., Tomas, R., Alexander, M. & Lawrence, D. The seasonal atmospheric response to projected Arctic Sea ice loss in the late twenty-first century. *J. Clim.* **23,** 333–351 (2010).
23. Overland, J. E., Wood, K. R. & Wang, M. Y. Warm Arctic-cold continents: Climate impacts of the newly open Arctic Sea. *Polar Res.* **30,** 15787 (2011).
24. Hopsch, S., Cohen, J. & Dethloff, K. Analysis of a link between fall Arctic sea ice concentration and atmospheric patterns in the following winter. *Tellus A* **64,** 18624 (2012).
25. Scaife, A. A. *et al.* Skillful long-range prediction of European and North American winters. *Geophys. Res. Lett.* **41,** 2514–2519 (2014).
26. Budikova, D. Role of Arctic sea ice in global atmospheric circulation: A review. *Glob. Planet. Change* **68,** 149–163 (2009).
27. Dee, D. P. *et al.* The ERA-Interim reanalysis: Configuration and performance of the data assimilation system. *Q. J. R. Meteorol. Soc.* **137,** 553–597 (2011).
28. Takaya, K. & Nakamura, H. Geographical dependence of upper-level blocking formation associated with intraseasonal amplification of the Siberian high. *J. Atmos. Sci.* **62,** 4441–4449 (2005).
29. Zhang, Y., Sperber, K. R. & Boyle, J. S. Climatology and interannual variation of the East Asian Winter Monsoon: Results from the 1979–95 NCEP/NCAR Reanalysis. *Mon. Weath. Rev.* **125,** 2605–2619 (1997).
30. Sato, K., Inoue, J. & Watanabe, M. Influence of the Gulf Stream on the Barents Sea ice retreat and Eurasian coldness during early winter. *Environ. Res. Lett.* **9,** 084009 (2014).
31. Renwick, J. A. & Wallace, J. M. Relationships between North Pacific wintertime blocking, El Nino, and the PNA pattern. *Mon. Weath. Rev.* **124,** 2071–2076 (1996).
32. Cowtan, K. & Way, R. G. Coverage bias in the HadCRUT4 temperature series and its impact on recent temperature trends. *Q. J. R. Meteorol. Soc.* **140,** 1935–1944 (2014).

Acknowledgements

J.-S.K. was supported by National Research Foundation (NRF-2014R1A2A2A01003827). J.-H.J. was supported by Korea Polar Research Institute project (PE15010). B.-M.K. was supported by Korea Meteorological Administration Research and Development Program (KMIPA2015-2093). C.K.F. was supported by the Joint UK DECC/Defra Met Office Hadley Centre Climate Programme (GA01101).

Author contributions

J.-S.K. and J.-H.J. designed the research, conducted analyses, and wrote the majority of the manuscript content. B.-M.K., C.K.F., S.-K.M. and S.-W.S. conducted the analysis and report-writing tasks. Y.-S.J. conducted analyses, numerical experiments and prepared figures. All the authors discussed the study results and reviewed the manuscript.

Additional information

Supplementary information is available in the online version of the paper. Reprints and permissions information is available online at www.nature.com/reprints. Correspondence and requests for materials should be addressed to J.-H.J.

Competing financial interests

The authors declare no competing financial interests.

Methods

Data and statistics. The linear trends of SAT, as shown in Fig. 1, are calculated from interpolated median version HadCRUT4 data (http://www.metoffice.gov.uk/hadobs/hadcrut4/data/current/download.html), hybridized with the University of Alabama in Huntsville (UAH) satellite data[32] (http://www-users.york.ac.uk/~kdc3/papers/coverage2013/series.html) for the period 1979 to 2014. The monthly- and daily-mean SAT, wind, geopotential height and SLP from 1979 to 2014 are obtained from the ERA-Interim Reanalysis[27] (http://apps.ecmwf.int/datasets/data/interim_full_daily). All analyses in Figs 2–4 are conducted after removing linear trends. The significance test used in this study is based on a standard two-tailed t-test in Figs 2, 3 and Supplementary Figures, with the number of degrees of freedom estimated by calculating autocorrelations. We also use a Monte Carlo approach using a bootstrap method to estimate internal variability in Fig. 4. For each model simulation, we randomly select 100 years from the historical simulation, calculate the regression coefficient using the selected 100 years, and finally compute the distribution of the regression coefficients by repeating this process 1,000 times. For MME, 39 regression coefficients are randomly selected from the 39 models, and their average is computed. By repeating this process 1,000 times, the distribution of MME is computed.

Model experiments. The GFDL CM2.1 model is used for the idealized coupled GCM experiment, developed by the Geophysical Fluid Dynamics Laboratory. To examine the impact of Arctic warming/cooling, SST in high latitudes (north of 70° N) is restored to the historical observed SST for 1950–2013, with a five-day restoring timescale, whereas the model is fully coupled over the other regions. ERSST v3 (http://www.esrl.noaa.gov/psd/data/gridded/data.noaa.ersst.html) is used for the observed SST. A total of six ensemble simulations with different initial conditions are carried out. The initial conditions were randomly chosen from long-term climate simulations under present-day climate conditions.

Analysis of CMIP5 data. We analyse the 39 CGCM simulations from the historical runs available in the CMIP5 archives (http://cmip-pcmdi.llnl.gov/cmip5/data_portal.html), reflecting transient climate conditions which include observed atmospheric composition due to both anthropogenic and natural sources. For a fair comparison, we used only one ensemble member from each model. Model references, details of the institutions where the models were run, and integration periods are summarized in Supplementary Table 1.

Code availability. We have opted not to make the computer code associated with this paper available because all the codes are for well-known statistical calculations.